

Global Dynamical Structure Reconstruction from Reconstructed Dynamical Structure Subnetworks: Applications to Biochemical Reaction Networks

Enoch Yeung, Jongmin Kim, Jorge Gonçalves, and Richard M. Murray

Abstract—In this paper we consider the problem of network reconstruction, with applications to biochemical reaction networks. In particular, we consider the problem of global network reconstruction when there are a limited number of sensors that can be used to simultaneously measure state information. We introduce dynamical structure functions as a way to formulate the network reconstruction problem and motivate their usage with an example physical system from synthetic biology. In particular, we argue that in synthetic biology research, network verification is paramount to robust circuit operation and thus, network reconstruction is an invaluable tool. Nonetheless, we argue that existing approaches for reconstruction are hampered by limited numbers of biological sensors with high temporal resolution. In this way, we motivate the global network reconstruction problem using partial network information and prove that by performing a series of reconstruction experiments, where each experiment reconstructs a subnetwork dynamical structure function, the global dynamical structure function can be recovered in most cases. We illustrate these reconstruction techniques on a recently developed four gene biocircuit, an event detector, and show that it is capable of differentiating the temporal order of input events.

I. INTRODUCTION

Two key variables that often determine the behavior of a dynamical system are its network structure and parametric realization. The structure of the network generally is determined by how states in the system causally depend on each other; edges in the network are determined by causal dependence while nodes are determined by the states of the system. Network structure alone does not determine dynamical behavior, though, parametric information is also important in determining what dynamical behaviors a system can achieve. Rather, network structure, or topology, often defines or narrows the possible behaviors a system can achieve. Without any structural constraints, a dynamical system can have arbitrary input-output behavior. Once network structure is imposed, the set of realizable input-output trajectories can be reduced.

This is particularly evident in biological networks; certain network topologies are referred to as network motifs [3]. In systems and synthetic biology, these network motifs are broadly accepted as enabling useful dynamical behavior. For example, an incoherent feed forward loop can be used for fold-change detection or adaptation, a cyclic network of repressors is associated with either oscillations or multistability, and a dual negative feedback network of two nodes is used as memory module or toggle switch. Network structure is thus an important aspect of designing synthetic biological circuits. By selecting an appropriate network motif and validating its functionality in practice, synthetic biolo-

gists are able to guide the phenotype of biological systems to match desired performance specifications.

It thus seems that the choice of network structure between engineered systems or even fundamental physical components is an important design variable to be considered. How components are interconnected implicitly defines network structure, which in turn constrains dynamical behavior of the system. Certain network structures can give rise to undesirable dynamic behavior [4]. Choosing the right network structure is thus an important problem in the synthesis of robust engineered dynamical systems.

Similarly, once a dynamical system has been designed and implemented, verifying that the network structure of a dynamical system is operating as designed is an equally important problem. This is especially critical, when the engineered system does not behave as expected (a pervasive challenge in current efforts to implement synthetic biocircuits) [5]. The problem of verifying or reverse-engineering a system's network structure from measurement data is called a network reconstruction problem. Network reconstruction problems are a specific class of system identification problems, where the model class of interest not only encodes parametric but structural information. In the next section we motivate and formulate the network reconstruction problem for different network representation models and argue that one particular representation is well suited for biochemical reaction networks: the dynamical structure function.

II. MOTIVATION: RECONSTRUCTING REPRESENTATIONS OF NETWORK STRUCTURE

The network structure of nonlinear dynamical systems is often implicitly defined by the state-space realization. Thus, the process of network reconstruction for the full system becomes a nonlinear parameter estimation or state-space realization problem. Such network reconstruction problems are non-convex, only locally identifiable at best, underconstrained due to the sampling limits of experimental data, and even ill-posed at times.

A class of dynamical systems where the concept of network structure is well-defined and reconstruction results are readily available are linear time-invariant (LTI) dynamical systems. The most intricate description of network structure of LTI systems refers to the network defined by interactions between every state in the system. Reconstructing the system's network structure is equivalent to finding a unique solution for the state-space realization. It is well known that uniquely determining the state-space realization,

is expensive, since it requires full-state feedback to be well-posed. It is thus valuable to find different representations of network structure, consistent with the state-space realization, that encode essential structural information, but that impose less stringent constraints on network reconstruction.

Arguably the simplest yet most broadly employed representation of network structure is the system transfer function. The transfer function describes the closed-loop causal dependencies of system outputs on system inputs. As such, it imposes weak information constraints on the process of network reconstruction; as long as it is possible to perturb the system with each input (not necessarily independently) and measure each output, it is possible to reconstruct the transfer function of the system. However, the transfer function contains very little structural information; the price of relatively relaxed constraints on the network reconstruction problem is that very little information about the actual network structure of the system, e.g. how states in the system depend on each other and interact, is encoded in the transfer function.

The tradeoffs between cost of network reconstruction and the “informativity” of the structural representation are especially clear in synthetic and systems biology research. In this area, finding or verifying the network of a biological system is an important problem. However, discovering the entire chemical reaction network is typically an ill-posed problem, since additional reactions may be introduced due to host or environmental context, loading effects, or unanticipated retroactivity effects [6]. Even without these effects, the reconstruction problem is equivalent to finding a unique realization for the dynamical system, which is ill-posed without measurements of every chemical species in the system. On the other hand, there are many inputs that can be used to perturb the system of interest, e.g. silencing RNA, genetic knock-outs, and small chemical inducers. Using these inputs, it is straightforward to reconstruct the transfer function of the system. However, the transfer function contains virtually no information about how chemical species within the system are interacting.

An intermediate representation of network structure that addresses this trade-off is the dynamical structure function [1]. It is a richer description of network structure than the transfer function since it models the causal interactions between measured outputs, in addition to the causal dependencies of outputs on input variables. At the same time, it does not require complete state feedback for reconstruction, since it only models the interactions among output states. In biological systems, this is especially applicable since the output variables of a system are also a subset of the state variables. All unmeasured states are subsumed in the edge-weight functions that describe interactions between measured variables. It is thus possible to experimentally target specific chemical species to measure and verify that the network structure of a biological system is functioning as intended.

A. The Dynamical Structure Function of an Incoherent (and Coherent) Feed-Forward Loop

To illustrate the utility of the dynamical structure function, consider the following design problem: to design and implement a novel incoherent feed-forward loop in a resource-limited environment. The traditional approach, unaided by the verification of network reconstruction, would assume that the physical binding interactions of select chemical species would be sufficient to enforce an incoherent feed-forward logic. Specifically, we consider implementing a feed-forward loop using the synthetic parts pLac-LasR-CFP-LVA, pLas-TetR-YFP-LVA, and pLas-Tet-RFP-LVA and IPTG, $C_3O_6H_{12} - HSL$, and aTc as inputs. A simple model for this system without any loading effects is given as:

$$\begin{aligned}
 \dot{x}_1 &= \rho_1 m_1 - \delta_p x_1 \\
 \dot{x}_2 &= \rho_2 m_2 - \delta_p x_2 \\
 \dot{x}_3 &= \rho_3 m_3 - \delta_p x_3 \\
 \dot{m}_1 &= \frac{\alpha_1 u_1}{k_{M,u1} + u_1} - \delta_m m_1 \\
 \dot{m}_2 &= \frac{\alpha_2 (x_1 u_2 / k_{M,u2})}{1 + x_1 / k_{M,1} + x_1 u_2 / k_{M,u2}} - \delta_m m_2 \\
 \dot{m}_3 &= \frac{\alpha_3 x_1 u_2}{1 + x_1 u_2 / k_{M,u2} + x_2 / (k_{M,2} + u_3 / k_{M,u3})} - \delta_m m_3 \\
 y &= \begin{bmatrix} \mathbf{I}_{3 \times 3} & \mathbf{0}_{3 \times 3} \end{bmatrix} \begin{bmatrix} \vec{x}^T & \vec{m}^T \end{bmatrix}^T
 \end{aligned} \tag{1}$$

The dynamical structure function for this system is derived by taking Laplace transforms and eliminating the hidden states m_1, m_2, m_3 , see [1] or [2] for a detailed derivation of dynamical structure functions. The network and control structure matrix transfer functions are written ($Q(s), P(s)$) where $Q(s)$ is written as

$$\begin{pmatrix} 0 & 0 & 0 \\ \frac{0.045}{s^2 + 1.5s + 5.7 \cdot 10^{-4}} & 0 & 0 \\ \frac{1.5 \cdot 10^{-4}}{s^2 + 1.7s + 0.2} & -\frac{1.5 \cdot 10^{-4}}{s^2 + 1.7s + 0.2} & 0 \end{pmatrix}.$$

We do not write out $P(s)$ here, however it is worth noting that $P(s)$ is a diagonal matrix and thus satisfies sufficient conditions for network reconstruction [1]. The network, with edge weight functions corresponding to the entries of $Q(s)$, is drawn in Figure 1A. Notice that if we take $s \in \mathbb{R}_{>0}$, the sign of the entries in $Q(s)$ coincides with the form of transcriptional regulation implemented by TetR and LasR, respectively. In [4] it was shown that the sign definite properties of entries in $Q(\mathbb{R}_{>0})$ are useful for reasoning about the monotonicity of interactions between measured outputs and how fundamental limits in system performance relate to network structure.

However, to truly prototype a novel feedforward loop, it is important to anticipate *in vivo* context effects. In this biocircuit, the components are particularly susceptible to loading effects [6]. In synthetic biological circuits, a protease called ClpXP targets and degrades LVA-tagged proteins. This protease can be found in limited supply when there are too many LVA-tagged proteins [7]. Modifying the above model

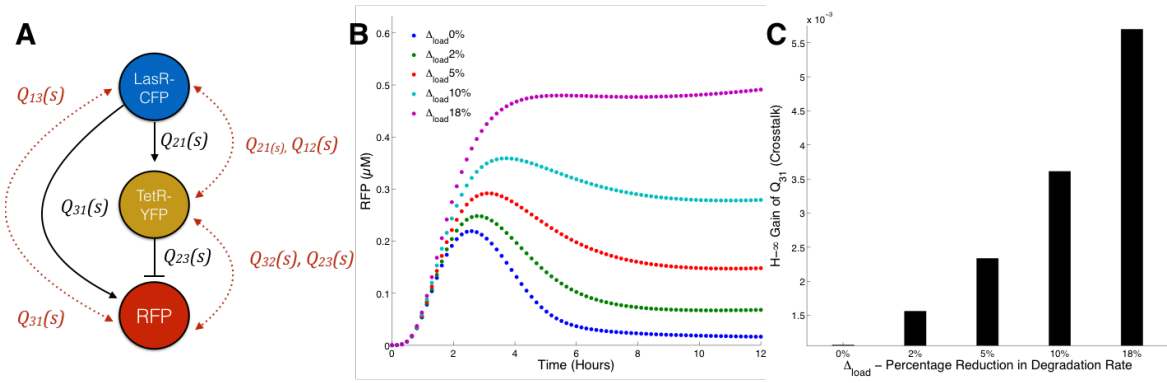


Fig. 1. **A** The dynamical structure of system (2). Nodes represent measured chemical species, with black edges denoting causal dependencies stemming from designed interactions, and red edges denoting causal dependencies arising from crosstalk or loading effects. Notice that the dynamical structure captures network models interactions that are not described by the system transfer function $G(s)$. **B** The input-output response of the nonlinear system (2). Standard parameters from the literature [8] were used to generate the simulation. As the size of the load Δ_{load} increases, the ability of the IFFL to respond with a pulse decreases. **C** The maximum fold-change in the H_∞ norm of the crosstalk entries in $Q(s)$. The H_∞ norm of $Q_{31}(s)$, plotted as a function of Δ_{load} . As the amplitude of directed crosstalk of x_1 (LasR-CFP) on x_3 (RFP) increases, the pulse height of RFP expression increases since the increased gain of Q_{31} allows RFP to achieve higher expression before TetR repression activates. However, the increase in crosstalk also means that TetR repression is less effective, resulting in steady-state drift as ClpXP load increases.

to account for these type of loading effects yields:

$$\begin{aligned}
 \dot{x}_1 &= \rho_1 m_1 - \frac{C_0 x_1 / k_{1,d}}{1 + x_1 / k_{1,d} + x_2 / k_{2,d} + x_3 / k_{3,d}} \\
 \dot{x}_2 &= \rho_2 m_2 - \frac{C_0 x_2 / k_{2,d}}{1 + x_1 / k_{1,d} + x_2 / k_{2,d} + x_3 / k_{3,d}} \\
 \dot{x}_3 &= \rho_3 m_3 - \frac{C_0 x_3 / k_{3,d}}{1 + x_1 / k_{1,d} + x_2 / k_{2,d} + x_3 / k_{3,d}} \\
 \dot{m}_1 &= \frac{\alpha_1 u_1}{k_{M,u1} + u_1} - \delta_m m_1 \\
 \dot{m}_2 &= \frac{\alpha_2 (x_1 u_2 / k_{M,u2})}{1 + x_1 / k_{M,1} + x_1 u_2 / k_{M,u2}} - \delta_m m_2 \\
 \dot{m}_3 &= \frac{\alpha_3 x_1 u_2 / k_{M,u2}}{1 + x_1 u_2 / k_{M,u2} + x_2 / (k_{M,2} + u_3 / k_{M,u3})} - \delta_m m_3 \\
 y &= [\mathbf{I}_{3 \times 3} \quad \mathbf{0}_{3 \times 3}] [\bar{x}^T \quad \bar{m}^T]^T
 \end{aligned} \tag{2}$$

Computing the dynamical structure function, we obtain $Q(s)$

$$\begin{pmatrix}
 0 & \frac{1.6 \cdot 10^{-3}}{s + 2.1 \cdot 10^{-3}} & \frac{0.041}{s + 2.1 \cdot 10^{-3}} \\
 \frac{(1.6 \cdot 10^{-3})s + 0.048}{s^2 + 1.5s + 3.3 \cdot 10^{-3}} & 0 & \frac{0.041}{s + 2.1 \cdot 10^{-3}} \\
 \frac{(3.8 \cdot 10^{-4})s + 7.4 \cdot 10^{-4}}{s^2 + 1.6s + 0.13} & \frac{(3.8 \cdot 10^{-4})s + 4.4 \cdot 10^{-4}}{s^2 + 1.6s + 0.13} & 0
 \end{pmatrix}$$

Notice that $Q(s)$ is no longer lower-triangular, but fully connected. Introducing loading effects creates additional coupling between nodes in the network. If the coupling is significant, the *designed* network interactions of the incoherent feedforward loop are overcome by the *crosstalk* network interactions [9].

In Figure 1 we simulate $Q(s)$ for different amounts of ClpXP loading. We use the variable

$$\Delta_{load}(x_1, x_3) \equiv \frac{(\Delta_c(x_1, x_3) - \Delta_{c,min}(x_1, x_3))}{\Delta_{c,min}(x_1, x_3)}$$

to denote the relative increase in loading effects from competition for ClpXP protease. We define the directed crosstalk of x_3 on x_1 as $\Delta_c(x_1, x_3)$, following the conventions in [9],

as

$$C_0 \int_0^T \frac{x_1 / k_{1,d}}{1 + x_1 / k_{1,d}} - \frac{x_1 / k_{1,d}}{1 + x_1 / k_{1,d} + x_2 / k_{2,d} + x_3 / k_{3,d}} dt.$$

Notice that from a design standpoint, the transfer function provides no insight into how to modify system structure to achieve better performance. If the first attempt to implement the feed-forward loop resulted in one of the non-pulsing traces, it would be unclear what component was the source of failure. Thus, current approaches for troubleshooting bio-circuits involve a systematic yet brute-force search over the design space.

Reverse-engineering the dynamical structure function allows us to discover unanticipated interactions between measured states. By targeting culprit edges revealed in network reconstruction, we reduce the complexity of the redesign problem to specific system components. In the case of system (2), for example, we find that $Q_{12}(s)$, $Q_{21}(s)$, $Q_{13}(s)$, $Q_{23}(s)$, $Q_{32}(s)$ and $Q_{31}(s)$ are the culprit (red) edges (c.f. Figure 1). The gain of these transfer functions increases as Δ_{load} increases as well. Additionally, the gain of these transfer functions is positively correlated with the binding strength of the LVA tags on x_1 and x_2 . Our simulation results suggest an intuitive way to attenuate loading effects — using weaker LVA tags of LasR and TetR (there are three different LVA tags, each with different binding affinity to ClpXP). Therefore, from a design standpoint, reverse-engineering the dynamical structure function of a system can provide critically valuable insight that could not be gleaned from estimating the system's transfer function. Network reconstruction is thus a powerful tool to aid network design of dynamical systems.

III. GLOBAL NETWORK RECONSTRUCTION FROM PARTITIONED SUBNETWORKS

Recall that necessary and sufficient conditions for dynamical structure function reconstruction were derived in [1]. However, the conditions stipulate that each vertex in

the network must be measured simultaneously over time. In synthetic biology, this is a reasonable requirement when reconstructing small networks comprised of two or three nodes, since three bimolecular reporters can be used to measure state dynamics (with minimal crosstalk between reporters). For larger networks comprised of many states, sequencing and microarray techniques yield low-temporal resolution data but such data is insufficient for dynamical structure reconstruction [1]. More broadly, in other physical applications, it may not always be possible to measure every single node in the dynamical structure network, even though it may be possible to perturb each one. By adjusting sensor placement, however, it may be possible to different snapshots of the global network. The question is whether these snapshots can be combined to reconstruct the global network, thereby extending the results of [1].

Additionally, it is often the case that a reconstructed network will reveal new pathways that merit further study. Zooming in on these pathways is equivalent to reconstructing a subnetwork of previously hidden states. Because of limited sensors, zooming in often means obscuring other measured states. Thus, it is important to understand how novel results of a previously hidden pathway should be integrated with existing network models of the larger global network.

To address this question, we first consider scenarios where a global network has been partitioned into two subnetworks, each of which are estimated in turn using the standard network reconstruction algorithm (the general case for n networks is similar but notation heavy). We will suppose that we have the ability to perturb each of the nodes in the global network, following the conditions outlined in [1]. For simplicity, we thus assume that each (measurable) species y_i in Y in the global network can be controlled independently (but not necessarily directly) using some input u_i in U , though such an assumption can be potentially relaxed [2]. We assume that the global system has a network modeled by dynamical structure function $(Q_b(s), P_b(s))$ which can be partitioned into two subnetworks (the general case follows by induction), commensurate with a partition on the vector Y into $Y = [Y_1 \ Y_2]^T$, written as

$$\begin{bmatrix} Y_1 \\ Y_2 \end{bmatrix} = \begin{bmatrix} Q_{b,11} & Q_{b,12} \\ Q_{b,21} & Q_{b,22} \end{bmatrix} \begin{bmatrix} Y_1 \\ Y_2 \end{bmatrix} + \begin{bmatrix} P_{b,1} & 0 \\ 0 & P_{b,2} \end{bmatrix} \begin{bmatrix} U_1 \\ U_2 \end{bmatrix} \quad (3)$$

where $Y_1 \in \mathbb{R}^{p_1}$ and $Y_2 \in \mathbb{R}^{p_2}$ and $U_1 \in \mathbb{R}^{m_1}$ and $U_2 \in \mathbb{R}^{m_2}$. Here we have omitted the argument s for each $Q_{b,i,j}$ and assume it is clear from context that we are working in the Laplace domain. From this equation, we can derive the following relation for (and the dynamical structure function of) $Y_1(s)$:

$$Y_1 = [Q_{b,11} + Q_{b,12}(I - Q_{b,22})^{-1}Q_{b,21}] Y_1 + P_{b,1}U_1 + Q_{b,12}(I - Q_{b,22})^{-1}P_{b,2}U_2 \quad (4)$$

We denote the subnetwork dynamical structure function for

Y_1 as $(Q_{s,1}, P_{s,1})$ where

$$\begin{aligned} Q_{s,1} &= (I - D_1)^{-1} (Q_{b,11} + Q_{b,12}(I - Q_{b,22})^{-1}Q_{b,21} - D_1) \\ P_{s,1} &= (I - D_1)^{-1} \left[\begin{array}{c|c} P_{b,1} & Q_{b,12}(I - Q_{b,22})^{-1}P_{b,2} \end{array} \right], \end{aligned} \quad (5)$$

$D_1 = \text{diag} [Q_{b,11} + Q_{b,12}(I - Q_{b,22})^{-1}Q_{b,21}]$ and $P_{s,1} \in \mathbb{R}^{p_1 \times p_1 + p_2}$ for each $s \in \mathbb{R}$. From [1], we know that number of inputs for the first subnetwork m_1 are the same as the number of outputs p_1 . Likewise, $m_2 = p_2$.

Notice that the subnetwork $(Q_{s,1}, P_{s,1})$ describing interactions between measured species Y_1 , assuming the measured species in Y_2 are hidden, is consistent with multiple global dynamical structure functions $(Q_b(s), P_b(s))$. Thus, simply using $(Q_{s,1}, P_{s,1})$ to identify $P_{b,1}$, $Q_{b,11}$ and $Q_{b,12}$ or $Q_{b,22}$ uniquely is impossible. In general, if D_1 is unknown, it is impossible to back out any of the terms $P_{b,1}$, $Q_{b,11}$ and $Q_{b,12}$ or $Q_{b,22}$.

An alternate path is to consider reconstruction of the second subnetwork and somehow combine the results to infer parameters of the first. If we consider the dynamical structure function for the subnetwork of measured species Y_2 , we get expressions for $(Q_{s,2}, P_{s,2})$

$$\begin{aligned} (I - D_2)^{-1} (Q_{b,22} + Q_{b,21}(I - Q_{b,11})^{-1}Q_{b,12} - D_2), \\ (I - D_2)^{-1} \left[\begin{array}{c|c} Q_{b,21}(I - Q_{b,11})^{-1}P_{b,1} & P_{b,2} \end{array} \right] \end{aligned} \quad (6)$$

where $D_2 \equiv \text{diag} [Q_{b,22} + Q_{b,21}(I - Q_{b,11})^{-1}Q_{b,12}]$ $Q_{s,2} \in \mathbb{R}^{p_2 \times p_2}$, $P_{s,2} \in \mathbb{R}^{p_2 \times p_1 + p_2}$ for each frequency s in \mathbb{C} . Notice that $Q_{b,22}$, $Q_{b,11}$, $Q_{b,12}$, $Q_{b,21}$ are all parameters that map to $Q_{s,2}$. The system is underdetermined, since it is a system of 6 equations with 8 unknown parameters, four in Q_b , two in P_b and the two diagonal matrices D_1 and D_2 . Thus, there is not enough information to reconstruct the global dynamical structure function from the sub dynamical structure functions. Unless additional information is known a priori, exact reconstruction of the global network is impossible.

Suppose, now that we have knowledge of D_1 and D_2 . Specifically, we consider the scenario when $D_1 = 0$ and $D_2 = 0$, i.e. when

$$Q_{s,1} = Q_{b,11} + Q_{b,12}(I - Q_{b,22})^{-1}Q_{b,21}$$

and

$$Q_{s,2} = Q_{b,22} + Q_{b,21}(I - Q_{b,11})^{-1}Q_{b,12}.$$

This raises the question, ‘‘What does it mean, structurally, for the matrices D_1 and D_2 are zero?’’ The answer can be explained as follows: D_1 is identically zero whenever the states of Y_2 are not part of any hidden state auto-regulatory loops for the states of Y_1 (and vice versa for D_2). We illustrate with an example.

A. Example: A Subsystem with No Hidden Autofeedback Loops

Suppose for simplicity that $Y_1 = [x \ y]^T$ and $Y_2 = [w \ z]^T$. First we consider the scenario where w is part of a negative feedback loop of x that involves another measured variable y from subnetwork containing x specifically, $x \rightarrow$

$w \rightarrow y \rightarrow x$. Here we use an arrow to denote dependence of the dynamics of one state on another.

We also suppose that $w \rightarrow z$; then the global network's topology is encoded by the global dynamical structure function as

$$Q_b(s) = \begin{bmatrix} 0 & Q_{xy}(s) & 0 & 0 \\ 0 & 0 & Q_{yw}(s) & 0 \\ Q_{wx}(s) & 0 & 0 & Q_{wz}(s) \\ 0 & 0 & Q_{zw}(s) & 0 \end{bmatrix} \quad (7)$$

and

$$Q_{b,11}(s) = \begin{bmatrix} 0 & Q_{xy}(s) \\ 0 & 0 \end{bmatrix}, \quad Q_{b,12} = \begin{bmatrix} 0 & 0 \\ Q_{yw}(s) & 0 \end{bmatrix}, \\ Q_{b,21} = \begin{bmatrix} Q_{wx}(s) & 0 \\ 0 & 0 \end{bmatrix}, \quad Q_{b,22} = \begin{bmatrix} 0 & Q_{wz}(s) \\ Q_{zw}(s) & 0 \end{bmatrix},$$

and from direct computation, we can write $Q_{b,11} + Q_{b,12}(I - Q_{b,22})^{-1}Q_{b,21}$ as

$$Q_{b,11} + \begin{bmatrix} 0 & 0 \\ Q_{yw}(s)Q_{wx}(s) & 0 \end{bmatrix} = \begin{bmatrix} 0 & Q_{xy}(s) \\ Q_{yw}(s)Q_{wx}(s) & 0 \end{bmatrix}$$

so $D_1 = [\mathbf{0}]$. Notice that the bottom left term in $Q_{s,1}$, namely $Q_{yw}Q_{wx}$, encodes the dynamics of w as a product of two transfer functions involving w to produce the open loop transfer function of x mapping to y . When w is a hidden (unmeasured) state, the effect of w on x in the auto-feedback loop is mediated by the measured variable y , thus, effectively, these hidden dynamics produce a causal dependency of one output variable y on another output variable x . If y was not measured, these hidden dynamics would create an auto-feedback loop on x , which would then result in D_1 being non-zero. When any variables from the second network (w or z) are involved in auto-feedback loops of one output variable in the first network (x), D_1 is non-zero if no other outputs from the first network are involved in the auto-feedback loop. Otherwise, D_1 is zero. ■

Thus, if we are provided a priori information that D_1 and D_2 are 0, then global network reconstruction is equivalent to finding $Q_{b,11}, Q_{b,12}, Q_{b,21}, Q_{b,22}, P_{b,1}, P_{b,2}$ from $Q_{s,1}, Q_{s,2}, P_{s,1}$, and $P_{s,2}$. If we partition $P_{s,1}$ and $P_{s,2}$ as

$$P_{s,1}(s) = [P_{s,11}(s) \mid P_{s,12}(s)]$$

and

$$P_{s,2}(s) = [P_{s,21}(s) \mid P_{s,22}(s)],$$

then we have the following relations:

$$\begin{aligned} P_{s,11} &= P_{b,1} \\ P_{s,12} &= Q_{b,12}(I - Q_{b,22})^{-1}P_{s,22} \\ P_{s,21} &= Q_{b,21}(I - Q_{b,11})^{-1}P_{s,11} \\ P_{s,22} &= P_{b,2} \\ Q_{s,1} &= Q_{b,11} + P_{s,12}P_{s,22}^{-1}Q_{b,21} \\ Q_{s,2} &= Q_{b,22} + P_{s,21}P_{s,11}^{-1}Q_{b,12} \end{aligned}$$

solving for $Q_{b,21} = P_{s,21}P_{s,11}^{-1}(I - Q_{b,11})$ and substituting $Q_{b,11} = Q_{s,1} - P_{s,12}P_{s,22}^{-1}Q_{b,21}$ yields

$$Q_{b,21} = (I - P_{s,21}P_{s,11}^{-1}P_{s,12}P_{s,22}^{-1})^{-1}P_{s,21}P_{s,11}^{-1}(I - Q_{s,1}).$$

Similarly, solving for $Q_{b,12} = P_{s,12}P_{s,22}^{-1}(I - Q_{b,22})$ and substituting $Q_{b,22} = Q_{s,2} - P_{s,21}P_{s,11}^{-1}Q_{b,12}$ yields

$$Q_{b,12} = (I - P_{s,12}P_{s,22}^{-1}P_{s,21}P_{s,11}^{-1})^{-1}P_{s,12}P_{s,22}^{-1}(I - Q_{s,2}).$$

Substituting these expressions for $Q_{b,12}$ and $Q_{b,21}$ respectively yields

$$\begin{aligned} Q_{b,11} &= Q_{s,1} - P_{s,12}P_{s,22}^{-1}(I - P_{s,21}P_{s,11}^{-1}P_{s,12}P_{s,22}^{-1})^{-1}X_{11} \\ Q_{b,22} &= Q_{s,2} - P_{s,21}P_{s,11}^{-1}(I - P_{s,12}P_{s,22}^{-1}P_{s,21}P_{s,11}^{-1})^{-1}X_{22} \\ X_{11} &= P_{s,21}P_{s,11}^{-1}(I - Q_{s,1}) \\ X_{22} &= P_{s,12}P_{s,22}^{-1}(I - Q_{s,2}). \end{aligned}$$

These expressions of $Q_{b,12}, Q_{b,21}$ and $Q_{b,11}, Q_{b,22}$ are uniquely determined by the known subnetwork matrices $Q_{s,1}, Q_{s,2}, P_{s,1}$, and $P_{s,2}$. Moreover, when $P_{s,11}$ and $P_{s,22}$ are diagonal, as per the recommended experimental setup in [1], their inverses can be computed exactly. Thus, when sufficient a priori information is available, exact global network reconstruction from reconstructed subnetworks is possible.

B. Investigating Global Boolean Reconstruction of Partitioned Subnetworks

In many situations, a priori information regarding the dynamical structure of D_1 and D_2 are not necessarily available. It is natural to wonder if it is possible to infer the Boolean structure of D_1 and D_2 , via Boolean reconstruction of the subnetworks of Y_1 and Y_2 . Since $I - D_1$ and $I - D_2$ are diagonal, it does not alter the Boolean structure any matrix it multiplies. In particular, we define the Boolean operator

$$\mathcal{B}(x) = \begin{cases} 1 & \text{if } x \neq 0 \\ 0 & \text{if } x \equiv 0 \end{cases}.$$

and note that when D_1 and D_2 are not assumed to be zero, then the full expression for $Q_{b,11}$ is written as

$$(I + K_1K_2)Q_{b,11} = (I - D_1)Q_{s,1} + K_1K_2 - D_1 \quad (8)$$

where

$$\begin{aligned} K_1 &= (I - D_1)P_{s,12}P_{s,22}^{-1}, \\ K_2 &= (I - D_2)P_{s,21}P_{s,11}^{-1}. \end{aligned} \quad (9)$$

When $P_{s,22}$ and $P_{s,11}$ are diagonal, as per the conditions of [1], and since D_1 and D_2 are diagonal matrices by definition, then any non-diagonal Boolean structure arises from the structure of $P_{s,12}$ and $P_{s,21}$. Thus,

$$\begin{aligned} \mathcal{B}(K_1) &= \mathcal{B}(P_{s,12}), \\ \mathcal{B}(K_2) &= \mathcal{B}(P_{s,21}). \end{aligned} \quad (10)$$

In general, for transfer function matrices $K_1(s)$ and $K_2(s)$,

$$\mathcal{B}(K_1K_2) \neq \mathcal{B}(K_1)\mathcal{B}(K_2).$$

There are ways in which non-zero rows of $K_1(s)$ and non-zero columns of $K_2(s)$ can multiply to produce an exact cancellation of non-zero transfer function entries. Additionally, in computing $Q_{b,11}$ there can be exact cancellations between the summation of $(I - D_1)Q_{s,1}$ and K_1K_2 . In practice, exact cancellations such as these are rare, since engineered physical systems that rely on exact cancellations typically are not stable or highly sensitive to perturbations. Nonetheless, in the next section we highlight a different class of subnetwork systems that can always be used for Boolean global dynamical structure reconstruction.

IV. GLOBAL RECONSTRUCTION USING OVERLAPPING SUBNETWORKS

In this section we visit the problem of reconstructing a global dynamical structure function from overlapping subnetwork estimates. Intuitively, there is shared information between subnetworks, since they share some of the observed states. Thus, is it possible to combine that information to reproduce an accurate global network structure?

Consider a dynamical system for which there are three groups of states $Y_1, Y_2, Y_3 \in \mathbb{R}^{p_1}, \mathbb{R}^{p_2}$, and \mathbb{R}^{p_3} respectively. Suppose that any pairwise combination of two groups can be measured at the same time, but not all three simultaneously. In the case of biochemical reaction networks, even though it is possible to measure three fluorescent proteins at once, it is common practice to use only two in order to avoid spectral crosstalk. In such a scenario, the networks are purposely monitored with the hope that overlapping measured states in each subnetwork makes Boolean and global dynamical structure reconstruction possible without any a priori information. The global dynamical structure function for such a system can be expressed generally as

$$Q_b = \begin{bmatrix} 0 & Q_{b,12} & Q_{b,13} \\ Q_{b,21} & 0 & Q_{b,23} \\ Q_{b,31} & Q_{b,32} & 0 \end{bmatrix}$$

and we assume a diagonal control structure with

$$P_b = \begin{bmatrix} P_{b,11} & 0 & 0 \\ 0 & P_{b,22} & 0 \\ 0 & 0 & P_{b,33} \end{bmatrix}.$$

If we consider the subnetwork just involving states Y_2, Y_3 and eliminate Y_1 as an output, we get internal structure Q_s^{23} which can be simplified to

$$(I - D_1)^{-1} \left(\begin{bmatrix} 0 & Q_{b,23} \\ Q_{b,32} & 0 \end{bmatrix} + \begin{bmatrix} Q_{b,21} \\ Q_{b,31} \end{bmatrix} \begin{bmatrix} Q_{b,12} & Q_{b,13} \end{bmatrix} - D_1 \right)$$

$$(I - D_1)^{-1} \left(\begin{bmatrix} Q_{b,21}Q_{b,12} & Q_{b,23} + Q_{b,21}Q_{b,13} \\ Q_{b,32} + Q_{b,31}Q_{b,12} & Q_{b,31}Q_{b,13} \end{bmatrix} - D_1 \right)$$

where

$$D_1 = \text{diag} \left(\begin{bmatrix} Q_{b,21}Q_{b,12} & Q_{b,23} + Q_{b,21}Q_{b,13} \\ Q_{b,32} + Q_{b,31}Q_{b,12} & Q_{b,31}Q_{b,13} \end{bmatrix} \right)$$

and control structure

$$P_s^{23} = (I - D_1)^{-1} \begin{bmatrix} Q_{b,21}P_{b,11} & P_{b,22} & 0 \\ Q_{b,31}P_{b,11} & 0 & P_{b,33} \end{bmatrix}$$

Notice that in this way of representing Q_s^{23} , the entries of Q_s^{23} are strictly proper, since $(I - D_1)^{-1}$ produces terms with relative degree 0. The subnetwork Q_s^{13} excluding Y_2 is

$$(I - D_2)^{-1} \left(\begin{bmatrix} Q_{b,12}Q_{b,21} & Q_{b,13} + Q_{b,12}Q_{b,23} \\ Q_{b,31} + Q_{b,32}Q_{b,21} & Q_{b,32}Q_{b,23} \end{bmatrix} - D_2 \right)$$

with

$$D_2 = \text{diag} \left(\begin{bmatrix} Q_{b,12}Q_{b,21} & Q_{b,13} + Q_{b,12}Q_{b,23} \\ Q_{b,31} + Q_{b,32}Q_{b,21} & Q_{b,32}Q_{b,23} \end{bmatrix} \right)$$

and

$$P_s^{13} = (I - D_2)^{-1} \begin{bmatrix} Q_{b,12}P_{b,22} & P_{b,11} & 0 \\ Q_{b,32}P_{b,22} & 0 & P_{b,33} \end{bmatrix}$$

The subnetwork Q_s^{12} excluding Y_3 is written as

$$(I - D_3)^{-1} \left(\begin{bmatrix} Q_{b,13}Q_{b,31} & Q_{b,12} + Q_{b,13}Q_{b,32} \\ Q_{b,21} + Q_{b,23}Q_{b,31} & Q_{b,23}Q_{b,32} \end{bmatrix} \right)$$

with

$$D_3 = \text{diag} \left(\begin{bmatrix} Q_{b,13}Q_{b,31} & Q_{b,12} + Q_{b,13}Q_{b,32} \\ Q_{b,21} + Q_{b,23}Q_{b,31} & Q_{b,23}Q_{b,32} \end{bmatrix} \right)$$

and

$$P_s^{12} = (I - D_3)^{-1} \begin{bmatrix} Q_{b,13}P_{b,33} & P_{b,11} & 0 \\ Q_{b,23}P_{b,33} & 0 & P_{b,22} \end{bmatrix}.$$

Without additional information, it is impossible to recover D_1, D_2, D_3 , and all the entries of Q and P simultaneously from the subnetworks alone. Like the partitioned network case, additional information must be obtained. However, unlike partitioned subnetworks, overlapping subnetworks are amenable to Boolean reconstruction. This in turn allows us to determine if D_1, D_2, D_3 are zero and whether global reconstruction of the dynamical structure is possible. To see how this follows, first note that the following equalities are true:

$$\begin{aligned} \mathcal{B}((I - D_1)^{-1}Q_{b,21}P_{b,11}) &= \mathcal{B}(Q_{b,21}P_{b,11}) & (11) \\ \mathcal{B}((I - D_1)^{-1}Q_{b,31}P_{b,11}) &= \mathcal{B}(Q_{b,31}P_{b,11}) \\ \mathcal{B}((I - D_2)^{-1}Q_{b,12}P_{b,22}) &= \mathcal{B}(Q_{b,12}P_{b,22}) \\ \mathcal{B}((I - D_2)^{-1}Q_{b,32}P_{b,22}) &= \mathcal{B}(Q_{b,32}P_{b,22}) \\ \mathcal{B}((I - D_3)^{-1}Q_{b,13}P_{b,33}) &= \mathcal{B}(Q_{b,13}P_{b,33}) \\ \mathcal{B}((I - D_3)^{-1}Q_{b,23}P_{b,33}) &= \mathcal{B}(Q_{b,23}P_{b,33}) \end{aligned}$$

Additionally, since $(I - D_i)$ is a strictly non-zero diagonal matrix, we have that $\mathcal{B}(I - D_i) = \mathcal{B}(I - D_i)(P_{b,ii})$ and since $P_{b,ii}$ are not identically zero, then $\mathcal{B}(Q_{b,ij})$ can be determined for $i \neq j$. Once we have $\mathcal{B}(Q_b(s))$ then it is possible to determine whether D_1, D_2 , or D_3 are zero.

If D_1, D_2, D_3 are zero then again, global dynamical reconstruction is possible. To see this, note that whenever D_1, D_2 , and D_3 are zero, the entries of $P_{b,11}, P_{b,22}, P_{b,33}$ can be read off of the reconstructed control structure matrices P_s^{13} and P_s^{23} respectively. Again, when $P_{b,11}, P_{b,22}$ and $P_{b,33}$ are diagonal, inversion of these transfer function matrices can be computed analytically (thus avoiding any functional

inversion issues). Then post-multiplying the P_s^{23} , P_s^{13} , and P_s^{12} with the inverses of $P_{b,11}$, $P_{b,22}$ and $P_{b,33}$ yields in the first column of each matrix:

$$\begin{aligned} P_s^{23} P_{b,11}^{-1} [1 : 2, 1] &= \begin{bmatrix} Q_{b,21} \\ Q_{b,31} \end{bmatrix}, \\ P_s^{13} P_{b,22}^{-1} [1 : 2, 1] &= \begin{bmatrix} Q_{b,12} \\ Q_{b,32} \end{bmatrix}, \\ P_s^{12} P_{b,33}^{-1} [1 : 2, 1] &= \begin{bmatrix} Q_{b,13} \\ Q_{b,23} \end{bmatrix} \end{aligned} \quad (12)$$

which thus completes reconstruction of Q_b .

V. CASE STUDY: GLOBAL DYNAMICAL NETWORK RECONSTRUCTION OF A TRANSCRIPTION-TRANSLATION EVENT DETECTOR

We have recently developed a novel event detector biocircuit in a cell-free transcription translation system [10], for performing temporal logic. The details of operation for this biocircuit are beyond the scope of this paper, but Figure 2 provides a visual summary. We thus summarize the key concepts as follows: a memory module comprised of states TetR (x_1) and LacI (x_3) implementing dual negative feedback retains the memory of the *past* arrival of inputs in the past. Two direct-readout states, CFP (x_2) and a far-red fluorescent protein (x_4) monitor the *present* arrival of inputs arabinose and HSL. A simple model for the system is given as follows

$$\begin{aligned} \dot{x}_1 &= \rho_1 m_1 - \delta_p x_1, \\ \dot{x}_2 &= \rho_2 m_2 - \delta_p x_2, \\ \dot{x}_3 &= \rho_3 m_3 - \delta_p x_3, \\ \dot{x}_4 &= \rho_4 m_4 - \delta_p x_4, \\ \dot{m}_1 &= \frac{k_1(k_l + u_5/k_{M,u5})}{(1 + x_3/k_{M,3} + u_1/k_{M,u1})} + u_1 - \delta_m m_1, \\ \dot{m}_2 &= \frac{k_2(k_l + u_5/k_{M,u5})}{(1 + u_5/k_{M,u5})} + u_2 - \delta_m m_2, \\ \dot{m}_3 &= \frac{k_3(k_l + u_6/k_{M,u6})}{(1 + x_1/k_{M,1} + u_2/k_{M,u2})} + u_3 - \delta_m m_3, \\ \dot{m}_4 &= \frac{k_4(k_l + u_6/k_{M,u6})}{(1 + u_6/k_{M,u6})} + u_4 - \delta_m m_4, \end{aligned} \quad (13)$$

We first construct three versions of the system with one version measuring states x_1 , x_2 , and x_3 and another version measuring states x_1 , x_3 , and x_4 . We have thus set up an overlapping subnetwork reconstruction problem, so that we can at least perform Boolean reconstruction. Here the global network consists of four nodes and four inputs (excluding arabinose and HSL), one for each node in the event detector network. We seek to determine all entries of $Q_b(s)$ and $P_b(s)$.

Let $Q_{s,[i_1:i_2]}$ denote the subnetwork dynamical structure function for states x_{i_1} to states x_{i_2} . The subnetwork for $Q_{s,[1:3]}$, and $Q_{s,[1,3:4]}$, are written as:

$$Q_{s,[1:3]} = \begin{pmatrix} 0 & 0 & -\frac{0.078}{d(s)} \\ 0 & 0 & 0 \\ -\frac{0.16}{d(s)} & 0 & 0 \end{pmatrix}$$

$$Q_{s,[1,3:4]}(s) = \begin{pmatrix} 0 & -\frac{0.078}{d(s)} & 0 \\ -\frac{0.16}{d(s)} & 0 & 0 \\ 0 & 0 & 0 \end{pmatrix} \quad (14)$$

The corresponding control subnetworks $P_{s,[1:3]}$ and $P_{s,[1,3:4]}$, are given as:

$$\begin{aligned} P_{s,[1:3]} &= \begin{pmatrix} d(s)\frac{1.3 \cdot 10^{-3}}{d(s)} & 0 & 0 & 0 \\ 0 & \frac{1.0 \cdot 10^{-3}}{d(s)} & 0 & 0 \\ 0 & 0 & \frac{1.5 \cdot 10^{-3}}{d(s)} & 0 \end{pmatrix} \\ P_{s,[1,3:4]} &= \begin{pmatrix} \frac{1.3 \cdot 10^{-3}}{d(s)} & 0 & 0 & 0 \\ 0 & 0 & \frac{1.5 \cdot 10^{-3}}{d(s)} & 0 \\ 0 & 0 & 0 & \frac{1.6 \cdot 10^{-3}}{d(s)} \end{pmatrix} \end{aligned}$$

Here we have written each P matrix with the convention that it is post-multiplied by u_i in ascending order. The first two $P(s)$ matrices have zero columns in their fourth and second columns respectively. Notice, since Q_b is zero on the diagonal, P_b is diagonal and non-zero in all diagonal entries, and $I - D_4 \neq 0$ (since D_4 consists of strictly proper transfer functions) then the equality to the fourth column of $P_{s,[1:3]}$

$$[0 \ 0 \ 0]^T = [Q_{b,14} \ Q_{b,24} \ Q_{b,34}]^T (I - Q_{b,44})^{-1} P_{b,44}$$

implies that $Q_{b,14}$, $Q_{b,24}$ and $Q_{b,34}$ are identically zero. Similarly, examining the second column of $P_{s,[1,3:4]}$ and noting that

$$[0 \ 0 \ 0]^T = [Q_{12} \ Q_{32} \ Q_{42}]^T (I - Q_{22})^{-1} P_{b,22}$$

allows us to conclude that $Q_{b,12}$, $Q_{b,32}$, and $Q_{b,42}$ are zero. Since $Q_{b,44} = 0$ it follows from the results in the previous section that $\mathcal{B}(Q_{s,[1:3]})$ can be written as

$$\mathcal{B} \left(\begin{bmatrix} 0 & Q_{b,12} & Q_{b,13} \\ Q_{b,21} & 0 & Q_{b,23} \\ Q_{b,31} & Q_{b,32} & 0 \end{bmatrix} + \begin{bmatrix} Q_{b,14} \\ Q_{b,24} \\ Q_{b,34} \end{bmatrix} \begin{bmatrix} Q_{b,41} \\ Q_{b,42} \\ Q_{b,43} \end{bmatrix}^T \right)$$

and in particular, applying the constraints above yields

$$\mathcal{B}(Q_{s,[1:3]}) = \mathcal{B} \left(\begin{bmatrix} 0 & Q_{b,12} & Q_{b,13} \\ Q_{b,21} & 0 & Q_{b,23} \\ Q_{b,31} & Q_{b,32} & 0 \end{bmatrix} \right)$$

We thus discover that $Q_{b,12}$, $Q_{b,21}$, $Q_{b,23}$, and $Q_{b,32}$ are all zero while $Q_{b,13}$ and $Q_{b,31}$ are definitively non-zero. More importantly, the Boolean structure of Q_b is of the form

$$\begin{bmatrix} 0 & 0 & * & 0 \\ 0 & 0 & 0 & 0 \\ * & 0 & 0 & 0 \\ 0 & 0 & 0 & 0 \end{bmatrix}$$

which implies that D_4 is zero, so we can reconstruct the global dynamical structure function $Q_b(s)$. Reading off the entries in $Q_{s,[1:3]}$ we obtain the following final expression for

$$Q_b(s) = \begin{pmatrix} 0 & 0 & -\frac{0.078}{d(s)} & 0 \\ 0 & 0 & 0 & 0 \\ -\frac{0.16}{d(s)} & 0 & 0 & 0 \\ 0 & 0 & 0 & 0 \end{pmatrix}$$

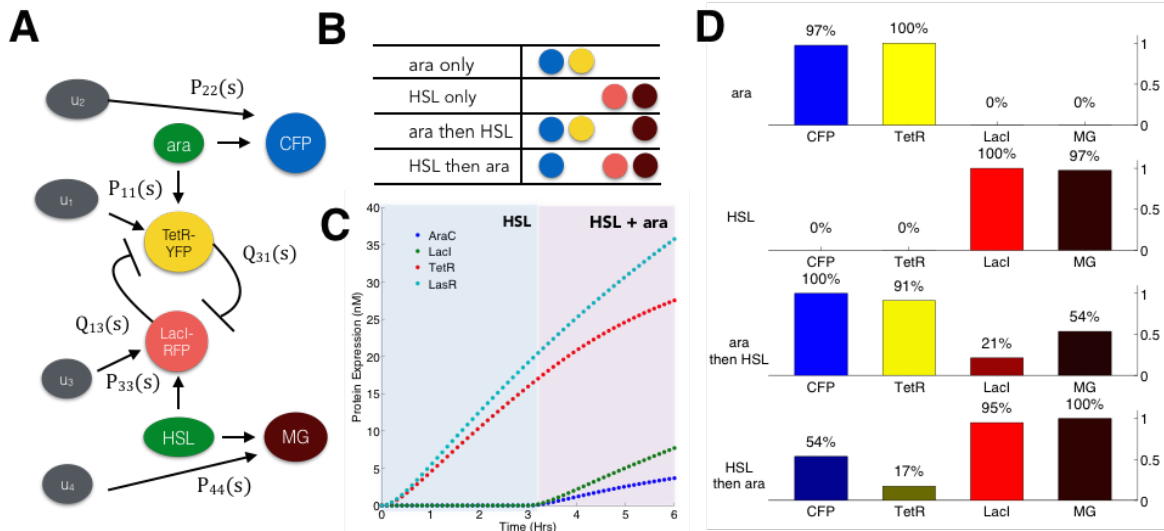


Fig. 2. **A** An event detector biocircuit comprised of a toggle switch and two direct-readout reporters. The toggle switch acts as a memory module while the direct-read out reporters report the current input state. **B** A table showing the ideal optical signature of the functional event detector, for each sequence of inputs. **C** A sample time-trace of the event detector in response to a sequential step input of HSL and then arabinose, modeled and simulated as system (13). **D** Steady-state simulation response of the functional event detector at $t = 6$ hours (cross-reference with table B). All simulation parameters were selected using biologically realistic ranges, as provided by the Harvard Bionumbers database [8].

while reading off the entries of $P_{s,[1:3]}$ and $P_{s,[1,3:4]}$ gives the control structure,

$$P_b(s) = \begin{pmatrix} \frac{1.3 \cdot 10^{-3}}{d(s)} & 0 & 0 & 0 \\ 0 & \frac{1.0 \cdot 10^{-3}}{d(s)} & 0 & 0 \\ 0 & 0 & \frac{1.5 \cdot 10^{-3}}{d(s)} & 0 \\ 0 & 0 & 0 & \frac{1.6 \cdot 10^{-3}}{d(s)} \end{pmatrix}$$

Notice that the appropriate placement of sensors is critical to global network reconstruction of the event detector. The toggle switch is a feedback loop that can cause D_i to be nonzero if sensors are placed on the wrong states. Specifically, any subnetwork that does not place sensors on both x_1 and x_3 at the same time will produce a non-zero D_i , which makes dynamical structure reconstruction not possible.

VI. CONCLUSION AND ACKNOWLEDGMENTS

In conclusion, we have introduced and discussed the importance of network reconstruction research, as well as motivated the utility of reconstructing dynamical structure functions for understanding dynamical systems. We have shown, with an example system, that reconstructing a dynamical structure function provides valuable insight for biocircuit design and robustness — insight that would be impossible to gain from the transfer function. More importantly, we have made a case that reverse engineering structural information about a dynamical system can reduce the complexity of system redesign.

In general, global network reconstruction is not always possible, since the availability and communication bandwidth of sensors may be limited. We motivated the problem of using dynamical structure subnetworks to reconstruct the global dynamical structure function of a system and showed that for several classes of subnetwork systems, global reconstruction from subnetwork estimates is possible. We illustrated our

results with an novel event detector, a biocircuit that we have successfully prototyped in a cell-free system (data not shown) and are currently optimizing it using network reconstruction techniques.

Acknowledgments: This work was supported by the Engineering and Physical Sciences Research Council, the Luxembourg National Research Foundation, Air Force Office of Scientific Research, Grant FA9550-14-1-0060, the Defense Advanced Research Projects Agency, Grant HR0011-12-C-0065, the National Science Foundation, Grant 1317291, and the John and Ursula Kanel Charitable Foundation.

REFERENCES

- [1] J. Gonçalves and S. Warnick. “Necessary and Sufficient Conditions for Network Reconstruction of LTI Systems.” *IEEE Transactions of Automatic Control*, 2007.
- [2] J. Adebayo et al. “Dynamical structure function identifiability conditions enabling signal structure reconstruction.” *Decision and Control (CDC)*, 2012 IEEE 51st Annual Conference on. IEEE, 2012.
- [3] J. Tyson, K. C. Chen, and B. Novak. “Sniffers, buzzers, toggles and blinkers: dynamics of regulatory and signaling pathways in the cell.” *Current opinion in cell biology* 15.2 (2003): 221-231.
- [4] E. Yeung, J. Kim, and R. M. Murray. “Resource competition as a source of non-minimum phase behavior in transcription-translation systems.” *Decision and Control (CDC)*, 2013 IEEE 52nd Annual Conference on. IEEE, 2013.
- [5] S. Cardinale, and A. P. Arkin. “Contextualizing context for synthetic biology: identifying causes of failure of synthetic biological systems.” *Biotechnology journal* 7.7 (2012): 856-866.
- [6] D. Del Vecchio, A. J. Ninfa, and E. D. Sontag. “Modular cell biology: retroactivity and insulation.” *Molecular systems biology* 4.1 (2008).
- [7] N. A. Cookson, et al. “Queueing up for enzymatic processing: correlated signaling through coupled degradation.” *Molecular systems biology* 7.1 (2011).
- [8] R. Milo, et al. “BioNumbers: the database of key numbers in molecular and cell biology.” *Nucleic acids research* 38.suppl 1 (2010): D750-D753.
- [9] E. Yeung et al. “Quantifying crosstalk in biochemical systems.” *Decision and Control (CDC)*, 2012 IEEE 51st Annual Conference on. IEEE, 2012.
- [10] V. Noireaux, R. Bar-Ziv, and A. Libchaber. “Principles of cell-free genetic circuit assembly.” *Proceedings of the National Academy of Sciences* 100.22 (2003): 12672-12677.